BJP BRITISH JOURNAL OF PHARMACOLOGY

BPS BRITISH PHARMACOLOGICAL SOCIETY

British Journal of Pharmacology (2009), 157, 1203–1214

0007-1188/09
www.brjpharmacol.org

RESEARCH PAPER

Mammalian P2X7 receptor pharmacology: comparison of recombinant mouse, rat and human P2X7 receptors

Diana L Donnelly-Roberts, Marian T Namovic, Ping Han and Michael F Jarvis

Neuroscience Research, Global Pharmaceutical Research and Development, Abbott Laboratories, Abbott Park, IL, USA

Background and purpose: Acute activation of P2X7 receptors rapidly opens a non-selective cation channel. Sustained P2X7 receptor activation leads to the formation of cytolytic pores, mediated by downstream recruitment of hemichannels to the cell surface. Species- and single-nucleotide polymorphism-mediated differences in P2X7 receptor activation have been reported that complicate understanding of the physiological role of P2X7 receptors. Studies were conducted to determine pharmacological differences between human, rat and mouse P2X7 receptors.
Experimental approach: Receptor-mediated changes in calcium influx and Yo-Pro uptake were compared between recombinant mouse, rat and human P2X7 receptors. For mouse P2X7 receptors, wild-type (BALB/c) and a reported loss of function (C57BL/6) P2X7 receptor were also compared.
Key results: BzATP [2,3-O-(4-benzoylbenzoyl)-ATP] was more potent than ATP in stimulating calcium influx and Yo-Pro uptake at rat, human, BALB/c and C57BL/6 mouse P2X7 receptors. Two selective P2X7 receptor antagonists, A-740003 and A-438079, potently blocked P2X7 receptor activation across mammalian species. Several reported P2X1 receptor antagonists [e.g. MRS 2159 (4-[(4-formyl-5-hydroxy-6-methyl-3-[(phosphonooxy)methyl}-2-pyridinyl)azo]-benzoic acid), PPNDS and NF279] blocked P2X7 receptors. NF279 fully blocked human P2X7 receptors, but only partially blocked BALB/c P2X7 receptors and was inactive at C57BL/6 P2X7 receptors.
Conclusions and implications: These data provide new insights into P2X7 receptor antagonist pharmacology across mammalian species. P2X7 receptor pharmacology in a widely used knockout background mouse strain (C57BL/6) was similar to wild-type mouse P2X7 receptors. Several structurally novel, selective and competitive P2X7 receptor antagonists show less species differences compared with earlier non-selective antagonists.
British Journal of Pharmacology (2009) **157,** 1203–1214; doi:10.1111/j.1476-5381.2009.00233.x; published online 22 June 2009

A related article is published in this issue of *BJP* (Wareham *et al.*, pp. 1215–1224). To view this article visit http://www3.interscience.wiley.com/journal/121548564/issueyear?year=2009

Keywords: P2X7 Receptors; Ca^{2+} influx; pore formation; species differences

Abbreviations: 2MeSATP, 2-methylthioadenosine 5′-triphosphate; α,β-meATP, α,β-methylene adenosine 5′-triphosphate; AP_3A, P^1,P^3-di(adenosine-5′) triphosphate; AP_4A, P^1,P^4-di(adenosine-5′) tetraphosphate; AP_5A, P^1,P^5-di(adenosine-5′) pentaphosphate; AP_6A, P^1,P^6-di(adenosine-5′) hexaphosphate; ATPγS, adenosine 5′-[γ-thio]triphosphate tetralithium salt; BBG, Brilliant Blue G; BzATP, 2,3-O-(4-benzoylbenzoyl)-ATP; DPBS, Dulbecco's phosphate-buffered saline; FLIPR, fluorometric imaging plate reader; KN-62, 1-[N,O-bis (5-isoquinolinesulphonyl)-N-methyl-L-tyrosyl]-4-phenylpiperazine; MRS 2159, 4-[(4-formyl-5-hydroxy-6-methyl-3-[(phosphonooxy)methyl}-2-pyridinyl)azo]-benzoic acid; MRS 2179, 2′deoxy-N^6-methyl adenosine 3′,5′-diphosphate; PPADS, pyridoxal phosphate-6-azophenyl-2-4-disulphonic acid; PPNDS, pyridoxal-5′-phosphate-6-(2′-naphthylazo-6′-nitro-4′,8′-disulphonate); TNP-ATP, 2′,3′-O-(2,4,6-trinitrophenyl) adenosine 5′-triphosphate; Yo-Pro-1, 4-[(3-methyl-2(3H)-benzoxazolylidene) methyl]-1[3-(trimethylammonio)propyl]-diiodide

Correspondence: Michael F Jarvis, Abbott Laboratories, 100 Abbott Park Road, Building AP9A, Department R4PM, Abbott Park, IL 60064-6123, USA. E-mail: michael.jarvis@abbott.com
Category: Molecular and cellular pharmacology K
Received 22 December 2008; revised 15 January 2009; accepted 20 January 2009

Introduction

The P2X7 receptor is a member of a family of ligand-gated ion channels activated by extracellular ATP. The P2X7 receptor is the most divergent member of this family in regards to its molecular structure, expression and function (Jacobson *et al.*,

2002; North, 2002; Burnstock, 2007). Structurally, P2X7 receptors have a longer intracellular C-terminus-containing multiple putative interactions sites for lipopolysaccharide (Denlinger *et al.*, 2001), SH2 domains and α-actin (Kim *et al.*, 2001). P2X7 receptors are highly expressed on immune cells including glial cells, macrophages and other antigen-presenting cells (Surprenant *et al.*, 1996). Pharmacologically, P2X7 receptors require higher concentrations of ATP ($EC_{50} \geq 100\ \mu mol \cdot L^{-1}$) for activation compared with other P2X receptors, and 2,3-O-(4-benzoylbenzoyl)-ATP (BzATP) is approximately 30-fold more potent than ATP (Surprenant *et al.*, 1996; Bianchi *et al.*, 1999). Activation of P2X7 receptors rapidly opens a non-selective cation channel, and longer agonist exposure leads to the progressive formation of large cytolytic pores (allowing passage of ~900 Da molecules) through the plasma membrane (North, 2002). P2X7 receptor-mediated pore formation is dependent on an intact C-terminal tail and is inhibited by extracellular divalent cations (Rassendren *et al.*, 1997). It has been recently demonstrated that P2X7 receptor-mediated pore formation is dependent on downstream signalling events (Donnelly-Roberts *et al.*, 2004) and is associated with the recruitment of hemichannels to the cell surface (Pelegrin and Surprenant, 2006). In addition to pore formation, activation of P2X7 receptors also initiates the rapid maturation and release of IL-1β (Sanz and DiVirgilio, 2000; Dubyak, 2007).

Understanding the physiological role of P2X7 receptors has been complicated by significant species differences for available P2X7 agonists and antagonists (Anderson and Nedergaard, 2006). For example, KN-62 (1-[N,O-bis (5 - isoquinolinesulphonyl) - N - methyl - L - tyrosyl] - 4 - phenylpiperazine) is a potent antagonist for human P2X7 receptors but is inactive at rat P2X7 receptors (Humphreys *et al.*, 1998). Conversely, Brilliant Blue G (BBG) is a rat selective P2X7 receptor antagonist (Jiang *et al.*, 2000). An additional complication arises from the fact that some antagonists non-competitively block agonist activation of the receptor (e.g. KN-62) while others are weak irreversible antagonists (e.g. oxidized ATP, oATP) (Jacobson *et al.*, 2002). Because activation of P2X7 receptors leads to a variety of cellular events that are mediated by direct channel opening (e.g. calcium influx) as well as receptor-mediated intracellular signalling (e.g. p38 MAPK activation, calmodulin regulation, hemichannel recruitment), apparent *in vitro* pharmacological differences in P2X7 receptor-mediated effects are dependent on the assay end point, antagonist mechanism of action and host cell or cell type used in different studies (Donnelly-Roberts and Jarvis, 2007; Roger *et al.*, 2008).

Deletion of the P2X7 receptor gene in the C57BL/6 mouse has provided evidence that activation of P2X7 receptors may mediate some aspects of chronic inflammation (Solle *et al.*, 2001; Labasi *et al.*, 2002) as well as inflammatory and nerve injury-induced pain (Chessell *et al.*, 2005). However, interpretation of the phenotype of P2X7 (–/–) mice is complicated by a reported loss of function mutation at position 451 (P451L) of the deduced amino acid sequence of the C57BL/6 mouse P2X7 receptor (Adriouch *et al.*, 2002). The P451L mutation results in a marked decrease in the activity of ATP to induce P2X7 receptor-mediated changes in calcium influx and cytolytic pore formation (Adriouch *et al.*, 2002; Le Stunff *et al.*, 2004). The P2X7 receptor found in most mammalian species, including BALB/c mice, rats and humans has proline at position 451 (Adriouch *et al.*, 2002).

Recently, we have described several novel and highly selective antagonists (e.g. A-438079 and A-740003) that competitively block P2X7 receptor activation *in vitro* and produce anti-nociceptive effects *in vivo* (Honore *et al.*, 2006; McGaraughty *et al.*, 2007). Additionally, a number of suramin-derived antagonists have been reported that have activities at multiple P2X receptors (Kassack *et al.*, 2004). The present studies were undertaken to characterize the agonist and antagonist pharmacology of recombinant mouse, rat and human P2X7 receptors stably expressed in 1321N1 astrocytoma cells that are naturally unresponsive to ATP (Bianchi *et al.*, 1999). For mouse P2X7 receptors, both the wild-type (BALB/c) and P451L mutant (C57BL/6) mouse P2X7 receptors were studied.

Methods

Cloning of C57BL/6 and BALB/c mouse P2X7 receptors

Mouse P2X7 receptor cDNA was obtained by reverse transcriptase polymerase chain reaction (RT-PCR) from mouse fibroblast cell line LTK-1 total RNA using mP2X7 5′ end primer: 5′ GCC ACC ATG CCG GCT TGC TGC AG 3′ and mP2X7 3′ end primer: 5′ CTT TCA GTA GGG ATA CTT GAA GC 3′. The 1.8 kb RT-PCR product that was correspondent to the C57BL/6 variant of mouse P2X7 receptor (Leucine residue at amino acid 451, Genbank ID: AJ489296) was subcloned into pCR2.1 TOPO vector (Invitrogen, Grand Island, NY, USA) for sequence confirmation. To functionally express in mammalian cells, the EcoRI fragment of pCR2.1 TOPO-mP2X7 was subsequently inserted into pIRESneo vector (BD Biosciences Clontech, San Jose, CA, USA). The BALB/c variant of mouse P2X7 receptor that encoded Proline at amino acid position 451 was generated by site-directed mutagenesis reaction with a pair of oligos (mP2X7 BALB/c up: 5′ TCC ACG ACT CAC CCC CGA CTC CTG GAC AAT C 3′ and mP2X7 BALB/c dn: 5′ GAT TGT CCA GGA GTC GGG GGT GAG TCG TGG A 3′) by using QuikChange mutagenesis kit from Stratagene (LaJolla, CA, USA). Both mouse P2X7 receptor expression constructs were completely sequenced before transfection.

Transfection and stable cell line construction

Human astrocytoma 1321N1 cells (Bianchi *et al.*, 1999) were maintained in Dulbecco's modified Eagle's medium (DMEM) medium supplemented with 10% FBS, 2 $mmol \cdot L^{-1}$ glutamine and 1× penicillin-streptomycin. Twenty-four hours before transfection, cells were split into 6 cm tissue culture plate. Five micrograms of pIRESneo-mP2X7 (451P) or pIRESneo-mP2X7 (451L) plasmid DNA was transfected into the cells by using Lipofectamine reagent (Invitrogen) according to manufacturer's instructions. Forty-eight hours after transfection, cells were split 1:10 into selection medium containing 0.3 $mg \cdot mL^{-1}$ Geneticin (Invitrogen, CA). Geneticin-resistant colonies were picked 10 days after selection. Cell clones that stably expressed mouse P2X7 receptor protein were determined by Western Blot and immunofluorescence analyses by using a P2X7 receptor antibody (Chemicon, Temecula, CA, USA).

1321N1 human astrocytoma cells stably expressing the following recombinant receptors were maintained as previously described (Bianchi *et al.*, 1999; Lynch *et al.*, 1999). Briefly, 1321N1 cells expressing P2X1, P2X4, $P2Y_1$, $P2Y_2$ and mammalian P2X7 receptors were maintained in a humidified 5% CO_2 atmosphere at 37°C in DMEM containing 1% L-Alanyl-L-Glutamine, 1% antibiotic/antimycotic, 10% FBS and 300 $\mu g \cdot mL^{-1}$ Geneticin. P2X2 expressing cells were grown in DMEM containing 1% L-Alanyl-L-Glutamine, 1% antibiotic/antimycotic, 10% FBS and 100 $\mu g \cdot mL^{-1}$ hygromycin B. P2X2/3 expressing cells were maintained in growth medium containing 150 $\mu g \cdot mL^{-1}$ Geneticin and 75 $\mu g \cdot mL^{-1}$ hygromycin B.

Ca^{2+} influx fluorometric imaging plate reader assay

Agonist-induced Ca^{2+} dynamics were assessed in all cell lines using the Ca^{2+} chelating dye, Fluo-4, in conjunction with a fluorometric imaging plate reader (FLIPR; Molecular Devices, Sunnyvale, CA) as previously described (Bianchi *et al.*, 1999) with noted minor modifications. The cells were plated out the day before the experiment onto Poly-D-lysine-coated black 96-well plates (Becton-Dickinson, Bedford, MA, USA and Sigma, St. Louis, MO, USA). Cell concentrations were 5×10^6 cells per plate. Fluo-4 was dissolved in anhydrous dimethyl sulphoxide (DMSO) to a final concentration of 5 $\mu g \cdot mL^{-1}$ in Dulbecco's phosphate-buffered saline (DPBS). The dye was loaded onto the adherent cells, and the plates were centrifuged for 5 min at 182 *g*. Cells were loaded for at least 1 h, but not more than 3 h and kept in the dark at room temperature. After loading, the extracellular Fluo-4 was removed by washing with DPBS using a SkanWasher 400 (Molecular Devices, Sunnyvale, CA, USA). All compound solutions were prepared in DPBS. After the agonist addition, Ca^{2+} dynamics were recorded for 3 min. P2X receptor agonists and antagonists were tested at 11 different concentrations. Independent measurements of a positive control (100%) were performed on each plate in order to normalize values from plate to plate; 4 $\mu mol \cdot L^{-1}$ ATP was used as positive control for P2X1, P2X4 and P2Y1 receptors; 10 $\mu mol \cdot L^{-1}$ ATP was used as positive control for P2X2 and P2X2/3 receptors; 1 $\mu mol \cdot L^{-1}$ UTP was used for $P2Y_2$ receptors; 5 $\mu mol \cdot L^{-1}$ BzATP was used as positive control for human P2X7 receptors, 10 $\mu mol \cdot L^{-1}$ BzATP for rat P2X7 receptors and 150 $\mu mol \cdot L^{-1}$ BzATP for mouse P2X7 receptors. For measurement of antagonist activity, compounds were added to the cell plate and fluorescence data collected for 3 min before the addition of the agonist. Fluorescence data were collected for another 2 min after the agonist addition. For some studies, compounds were added to the cell plates 60 min prior to agonist addition. Controls used for normalization in the antagonist experiments were the same as those used for agonist experiments. Concentration–response data were analysed by using GraphPad Prism (San Diego, CA, USA). Estimates of mean ± SEM pEC_{50} or pIC_{50} values were obtained from a single curve fit of the pooled data (n = 4–6 individual experiments, run in duplicate).

Yo-Pro uptake assay

The FLIPR was also used to measure agonist-induced uptake of Yo-Pro dye (MW = 629) in the recombinant P2X7 receptor cell lines as previously described (Donnelly-Roberts *et al.*, 2004). Cells were plated the day before at a density of 1×10^6 cells per plate onto Poly-D-Lysine-coated black-walled 96-well plates to reduce light scattering. Prior to Yo-Pro dye addition, cells were rinsed twice with PBS without Mg^{2+} or Ca^{2+} ions, which have been shown to inhibit pore formation (North, 2002). The Yo-Pro iodide dye (1 $mmol \cdot L^{-1}$ in 100% DMSO) was diluted to a final concentration of 2 $\mu mol \cdot L^{-1}$ in PBS (w/o Mg^{2+} or Ca^{2+}) and then placed on the cells immediately prior to agonist addition, and dye uptake was measured for 1 h. Antagonists were added to cells at the same time as the Yo-Pro dye. For antagonist activity measurements, the percentage of maximal intensity was normalized to that induced by the peak value for BzATP activation and plotted against the compound concentration to calculate IC_{50} values and to control for plate-to-plate variability. Concentration–response data were analysed by using GraphPad Prism (San Diego, CA, USA). Estimates of mean ± SEM pEC_{50} or pIC_{50} values were obtained from a single curve fit of the pooled data (n = 4–6 individual experiments, run in duplicate).

Materials

The nomenclature used for describing the P2X receptors conforms to the *BJP* Guide to Receptors and Channels (Alexander *et al.*, 2008) and that proposed by the LIGC committee of IUPHAR (Jarvis and Khakh, 2009). The following were purchased from Sigma (St. Louis, MO, USA): BzATP; ATP; UTP; ADP; α,β-meATP, α,β-methylene adenosine 5′-triphosphate; 2MeSATP, 2-methylthioadenosine 5′-triphosphate; ATPγS, adenosine 5′-[γ-thio]triphosphate tetralithium salt; AMP; UDP; AP_3A, P^1,P^3-di(adenosine-5′) triphosphate; AP_4A, P^1,P^4-di(adenosine-5′) tetraphosphate; AP_5A, P^1,P^5-di(adenosine-5′) pentaphosphate; AP_6A, P^1,P^6-di(adenosine-5′) hexaphosphate; PPADS, pyridoxal phosphate-6-azophenyl-2-4-disulphonic acid; BBG; Cibacron Blue 3GA; suramin; PPNDS, pyridoxal-5′-phosphate-6-(2′-naphthylazo-6′-nitro-4′,8′-disulphonate); MRS 2159, 4-[(4-formyl-5-hydroxy-6-methyl-3-[(phosphonooxy)methyl}-2-pyridinyl)azo]-benzoic acid; MRS 2179, 2′deoxy-N^6-methyl adenosine 3′,5′-diphosphate; TNP-ATP, 2′,3′-O-(2,4,6-trinitrophenyl) adenosine 5′-triphosphate; Reactive Blue 2; caffeine; theophylline; mecamylamine; phenol red; oATP, periodate oxidized ATP; DMEM; L-Alanyl-L-Glutamine. The following were purchased from Tocris (Ellisville, MO): NF023, NF279 and NF449. KN-62 was purchased from Sigma and Tocris. Geneticin, DPBS, fetal bovine serum, hygromycin B and antibiotic/antimycotic were purchased from Gibco (Grand Island, NY, USA). Fluo-4, AM was obtained from Molecular Probes (Eugene, OR). Yo-Pro-1 [4-[(3-methyl-2(3H)-benzoxazolylidene) methyl]-1[3-(trimethylammonio) propyl]-diiodide] was purchased from Molecular Probes (Eugene, OR, USA).

Results

Functional expression of BALB/c and C57BL/6 mouse P2X7 receptors

Mouse BALB/c (Genbank seq. AJ489297) and C57BL/6 (Genbank seq. AJ89296) P2X7 receptors were cloned and

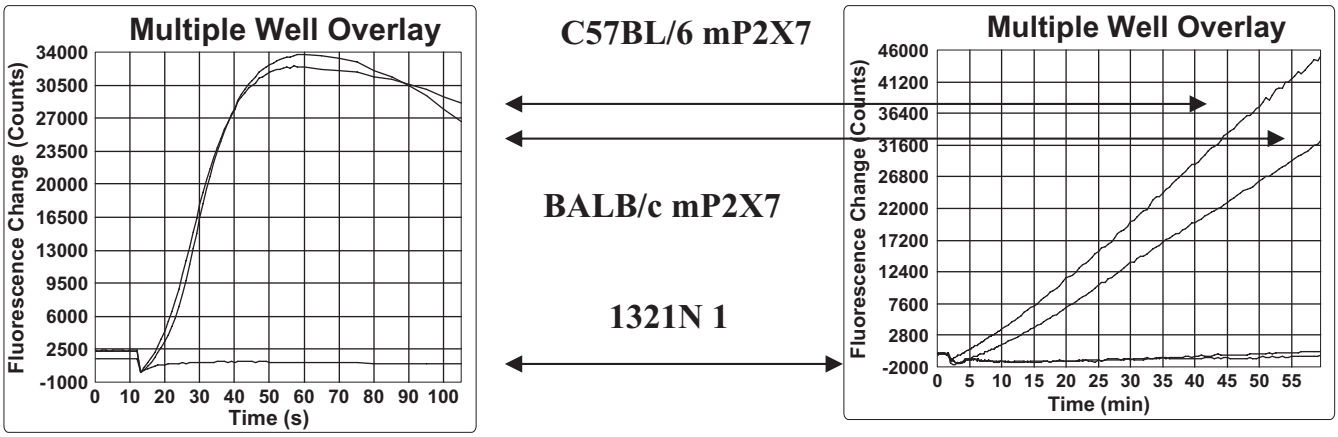

Figure 1 Representative fluorometric imaging plate reader tracings of BzATP [2,3-O-(4-benzoylbenzoyl)-ATP] (150 μmol·L^{-1})-stimulated calcium influx (left panel) and Yo-Pro uptake (right panel) in 1321N1 cells expressing BALB/c and C57BL/6 P2X7 receptors.

stably transfected into 1321N1 cells as confirmed by Western Blot analysis (data not shown). Application of BzATP (150 μmol·L^{-1}) to BALB/c and C57BL/6 mouse P2X7 receptors produced robust changes in intracellular calcium concentrations (Figure 1). The rate of calcium mobilization was similar for both mouse P2X7 receptors. BzATP did not significantly alter intracellular calcium mobilization in untransfected 1321N1 cells (Figure 1). The ability of BzATP to stimulate a time-dependent increase in Yo-Pro incorporation in cells expressing BALB/c or C57BL/6 P2X7 receptors was also similar (Figure 1).

Agonist activation of mammalian P2X7 receptors: [Ca^{2+}]$_i$

The ability of P2 receptor agonists to activate P2X7 receptor-mediated changes in intracellular calcium concentrations was compared across different mammalian species (Table 1; Figure 2). BzATP was the most potent agonist to activate P2X7 receptors and was fully efficacious in stimulating calcium influx across each species (Table 1). BzATP was 10-fold more potent to activate human and rat, as compared with the mouse P2X7 receptors (Table 1). ATP was 10–12-fold less potent than BzATP at human and mouse P2X7 receptors and was a partial agonist at the rat P2X7 receptor (Figure 2). The weak agonist efficacy of ATP in this study is consistent with previous data demonstrating that ATP is a low-efficacy agonist at native rat P2X7 receptors (Chen *et al.*, 2005). 2MeSATP and ATPγS were weakly potent full agonists for human P2X7 receptors and showed weak or no significant agonist activity at the other mammalian P2X7 receptors. A number of other purine and pyrimidine agonists for P2 receptors also displayed no agonist activity at P2X7 receptors at concentrations up to 1 mmol·L^{-1} (Table 1).

Agonist activation of mammalian P2X7 receptors: Yo-Pro uptake

BzATP was the most potent agonist to stimulate P2X7 receptor-mediated Yo-Pro uptake (Table 2; Figure 3). BzATP was most potent at human P2X7 receptors and was 10–100-fold weaker at the rat and mouse P2X7 receptors respectively (Table 2). ATP and ATPγS were 17- and 56-fold less potent respectively, as agonists compared with BzATP at the human receptor (Figure 3) and were less efficacious. These agonists showed either weak or no activity at the mouse P2X7 receptors (Table 2). While 2MeSATP was a fully efficacious agonist in stimulating human P2X7 receptor-mediated changes in intracellular calcium concentrations (Table 1), this agonist was ineffective in stimulating Yo-Pro uptake at concentrations up to 1 mmol·L^{-1} (Table 2). BzATP, ATP and ATPγS were more potent in stimulating human P2X7 receptor-mediated Yo-Pro uptake (Table 2) compared with their activities in the calcium influx assay (Table 1). A number of other purine and pyrimidine agonists for P2 receptors also displayed no agonist activity at P2X7 receptors at concentrations up to 1 mmol·L^{-1} (Table 2).

Antagonism of mammalian P2X7 receptors: [Ca^{2+}]$_i$

The ability of P2 receptor antagonists to block BzATP-stimulated changes in intracellular calcium concentrations was determined across the different species (Table 3). PPADS effectively blocked BzATP-mediated changes in intracellular calcium concentrations at mammalian P2X7 receptors and was more potent in blocking human and rat P2X7 receptors, as compared with mouse P2X7 receptors (Table 3). As previously demonstrated (Gargett and Wiley, 1997; Jiang *et al.*, 2000), the P2X7 receptor antagonists, KN-62 and BBG selectively blocked calcium influx only at the human and rat P2X7 receptors respectively (Table 3). These antagonists did not block mouse P2X7 receptors. The P2X1 receptor antagonist, NF279 blocked human P2X7 receptors in a concentration-dependent fashion. NF279, however, was less potent at blocking rat P2X7 receptors and only partially blocked BALB/c P2X7 receptors. NF279 was inactive at C57BL/6 P2X7 receptors (Table 3; Figure 4). Two previously reported P2X1 antagonists, PPNDS and MRS 2159 (Lambrecht, 2000; Kim *et al.*, 2001), potently blocked BzATP-mediated P2X7 receptor activation. These antagonists were approximately 10-fold more potent to block rat and human, as compared with mouse P2X7 receptors (Table 3). A-740003 and A-438079 showed significantly greater potency in blocking P2X7 receptor activation across all species compared with other antagonists (Figure 4). Like the other antagonists, A-740003 and A-438079

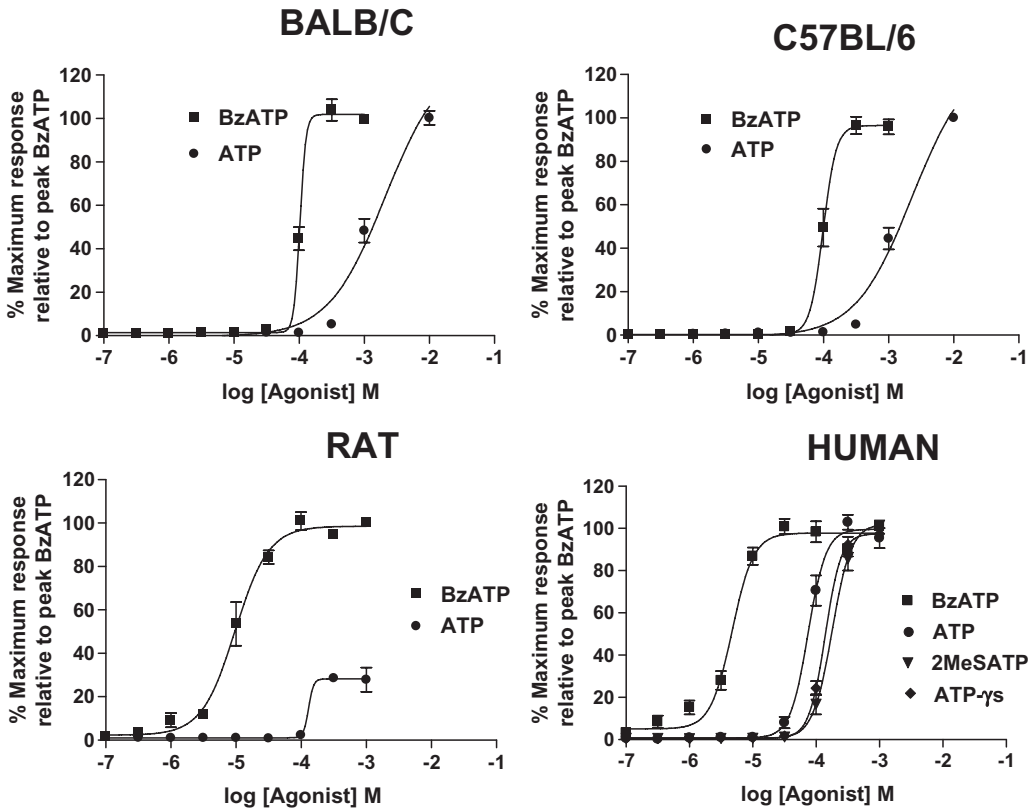

Figure 2 Agonist concentration–effect curves for P2 receptor agonists to stimulate increases in P2X7 receptor-mediated intracellular calcium concentrations. Data were normalized to the peak BzATP response (%Maximum response). Data represent mean ± SEM of 4–6 experiments. 2MeSATP, 2-methylthioadenosine 5′-triphosphate; ATPγS, adenosine 5′-[γ-thio]triphosphate tetralithium salt; BzATP, 2,3-O-(4-benzoylbenzoyl)-ATP.

Table 1 Activity of P2 receptor agonists to stimulate P2X7 receptor-mediated changes in intracellular calcium concentrations

Agonist	*Mouse P2X7, BALB/c*	*%Maximum efficacy*	*Mouse P2X7, C57BL/6*	*%Maximum efficacy*	*Rat P2X7*	*%Maximum efficacy*	*Human P2X7*	*%Maximum efficacy*
BzATP	3.99 ± 0.06	100	4.02 ± 0.02	100	5.01 ± 0.04	99	5.33 ± 0.05	98
ATP	2.62 ± 0.05	100	2.62 ± 0.05	100	3.89 ± 0.20	28	4.13 ± 0.02	100
2MeSATP	<3		<3		<3		3.75 ± 0.01	100
ATPγS	<3		<3		<3		3.86 ± 0.03	98

Data represent pEC_{50} ± SEM, $n = 4–6$ individual experiments. The following agonists did not produce a significant change in intracellular calcium concentrations at concentrations up to 1 mmol·L^{-1}: ADP, AMP, α,β-meATP, UTP, UDP, AP_3A, AP_4A, AP_5A and AP_6A.
2MeSATP, 2-methylthioadenosine 5′-triphosphate; α,β-meATP, α,β-methylene adenosine 5′-triphosphate; AP_3A, P^1,P^3-di(adenosine-5′) triphosphate; AP_4A, P^1,P^4-di(adenosine-5′) tetraphosphate; AP_5A, P^1,P^5-di(adenosine-5′) pentaphosphate; AP_6A, P^1,P^6-di(adenosine-5′) hexaphosphate; ATPγS, adenosine 5′-[γ-thio]triphosphate tetralithium salt; BzATP, 2,3-O-(4-benzoylbenzoyl)-ATP.

showed greater activity at rat and human, as compared with mouse P2X7 receptors (Table 3). Other P2X receptor antagonists evaluated were inactive at concentrations up to 100 μmol·L^{-1} (Table 3).

Antagonism of mammalian P2X7 receptors: Yo-Pro uptake

The ability of P2 receptor antagonists to block BzATP-stimulated Yo-Pro uptake was determined across the different species (Table 4). PPADS, and a number of reported P2X1 receptor antagonists including MRS 2159, NF023, NF279 and NF449, effectively blocked BzATP-stimulated Yo-Pro uptake at all mammalian P2X7 receptors (Table 4; Figure 5). Unlike their effects on P2X7 receptor-mediated calcium influx (Table 3), many of these antagonists showed either similar or slightly higher potency for blocking mouse P2X7 receptor-mediated Yo-Pro uptake compared with rat and human P2X7 receptors (Table 4). KN-62, a potent antagonist of human P2X7 receptors was inactive at the rat P2X7 receptor, but showed potent activity in blocking mouse P2X7 receptor-mediated Yo-Pro uptake (Figure 5). While BBG was only effective in blocking rat P2X7-mediated calcium influx (Table 3), this antagonist potently blocked P2X7-mediated Yo-Pro uptake and all mammalian P2X7 receptors (Table 4; Figure 5). Similarly, Cibacron Blue was inactive in blocking P2X7 receptor-mediated calcium influx but effectively blocked

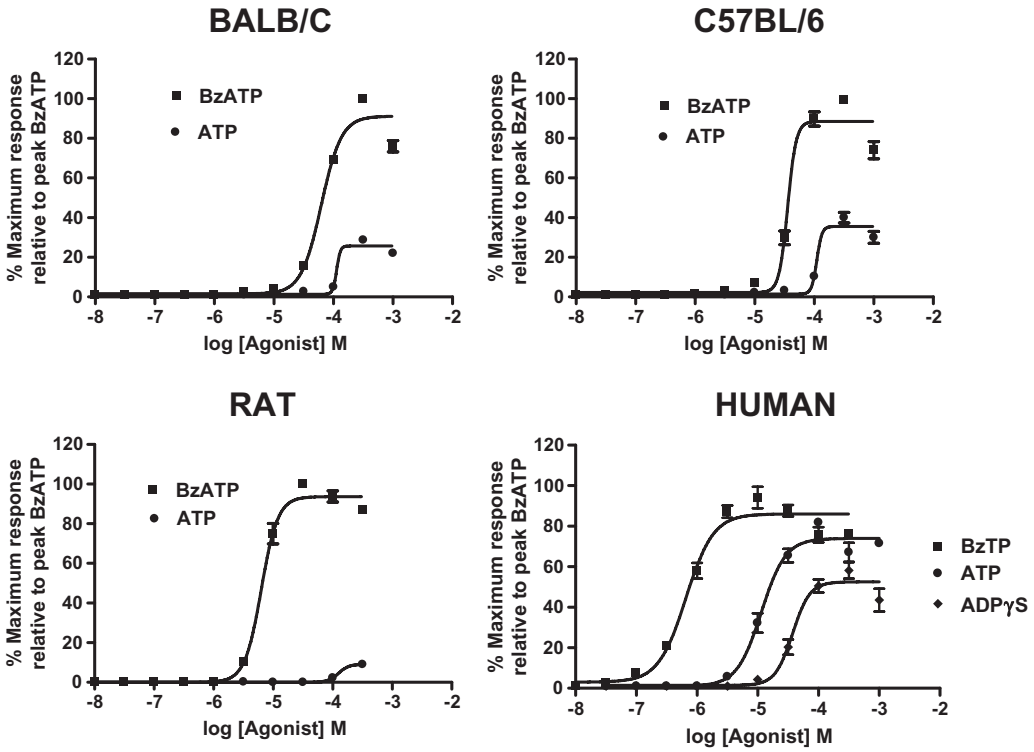

Figure 3 Agonist concentration–effect curves for P2 receptor agonists to stimulate an increase in P2X7 receptor-mediated Yo-Pro uptake. Data were normalized to the peak BzATP response (%Maximum response). Data represent mean ± SEM of 4–6 experiments. ATPγS, adenosine 5′-[γ-thio]triphosphate tetralithium salt; BzATP, 2,3-O-(4-benzoylbenzoyl)-ATP.

Table 2 Activity of P2 receptor agonists to stimulate P2X7 receptor-mediated Yo-Pro uptake

Agonist	*Mouse P2X7, BALB/c*	*%Maximum efficacy*	*Mouse P2X7, C57BL/6*	*%Maximum efficacy*	*Rat P2X7*	*%Maximum efficacy*	*Human P2X7*	*%Maximum efficacy*
BzATP	4.22 ± 0.08	100	4.44 ± 0.26	100	5.20 ± 0.03	100	6.18 ± 0.08	100
ATP	3.70 ± 0.14	25	3.79 ± 0.13	40	<4	9	4.94 ± 0.06	81
ATPγS	<3		<3		<3		4.43 ± 0.07	58

Data represents pEC_{50} ± SEM, $n = 4–6$ individual experiments. The following agonists did not produce a significant change in Yo-Pro uptake at concentrations up to 1 mmol·L^{-1}: ADP, AMP, α,β-meATP, 2MeSATP, ADPγS, UTP, UDP, AP_3A, AP_4A, AP_5A and AP_6A.
2MeSATP, 2-methylthioadenosine 5′-triphosphate; α,β-meATP, α,β-methylene adenosine 5′-triphosphate; AP_3A, P^1,P^3-di(adenosine-5′) triphosphate; AP_4A, P^1,P^4-di(adenosine-5′) tetraphosphate; AP_5A, P^1,P^5-di(adenosine-5′) pentaphosphate; AP_6A, P^1,P^6-di(adenosine-5′) hexaphosphate; ATPγS, adenosine 5′-[γ-thio]triphosphate tetralithium salt; BzATP, 2,3-O-(4-benzoylbenzoyl)-ATP.

P2X7 receptor-mediated Yo-Pro uptake across all species (Table 4). Reactive Blue 2 showed greater potency to block rat P2X7 receptors than at human or mouse P2X7 receptors. A-740003 and A-438079 were more potent in blocking rat P2X7 receptor-mediated Yo-Pro uptake compared with other antagonists (Table 4; Figure 5). While A-740003 showed equivalent potency to block human and rat P2X7 receptors, A-438079 was approximately 10-fold more potent at rat than at human and mouse P2X7 receptors (Table 3).

Extended incubation enhances P2X7 receptor antagonist potency: $[Ca^{2+}]_i$

The data shown in Tables 3 and 4 indicate that many antagonists were more potent in blocking BzATP-stimulated Yo-Pro uptake than in blocking BzATP-stimulated changes in intracellular calcium concentrations. Differences in agonist concentrations and/or the presence of divalent cations between the two assays may account for some of these differences. However, the assay incubation times also differ greatly between the two assays (3 min for calcium influx versus 60 min for Yo-Pro uptake). In order to address this difference, the antagonist preincubation time in the calcium influx assay was extended from 3 to 60 min. Table 5 shows the antagonist potencies for blocking BzATP-stimulated calcium influx at the 3 and 60 min pretreatment times. In general, the potency of most antagonists increased fourfold to eightfold following a 60 min preincubation compared with the 3 min preincubation. This difference was greater for KN-62 at the human and mouse P2X7 receptors (Table 5). KN-62 remained inactive at the rat P2X7 receptor. Extension of the assay incubation time also increased the potency of BBG at the rat P2X7 receptor, and this antagonist also effectively blocked mouse P2X7-mediated increases in intracellular calcium. A-740003 and

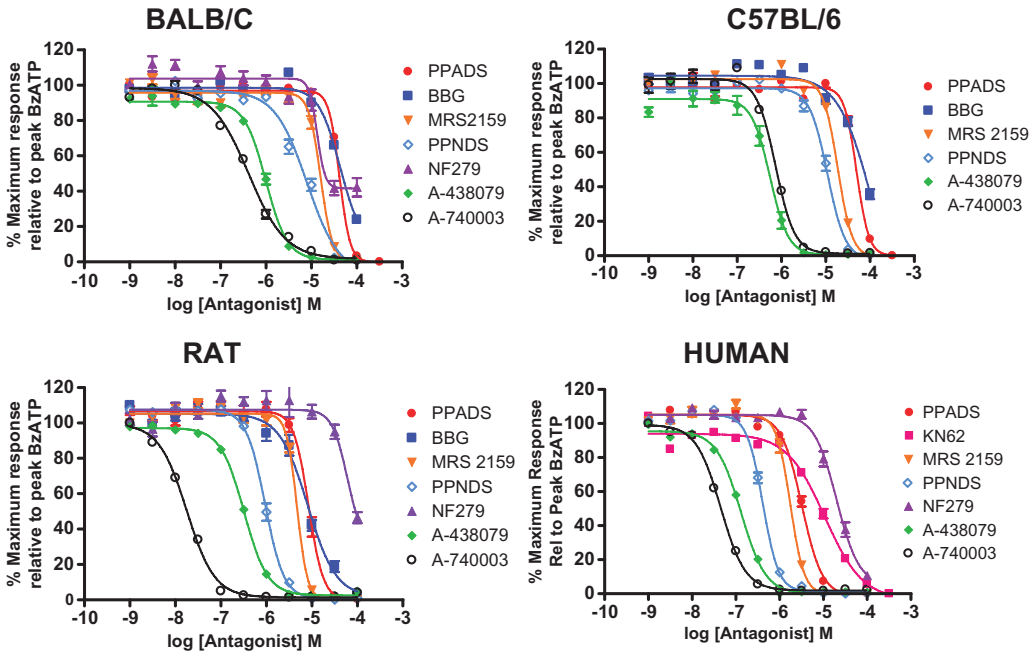

Figure 4 Concentration–effect curves for P2 receptor antagonists to block BzATP-stimulated increase in P2X7 receptor-mediated calcium influx. Data were normalized to the peak BzATP response (%Maximum response). Data represent mean ± SEM of 4–6 experiments. BBG, Brilliant Blue G; BzATP, 2,3-O-(4-benzoylbenzoyl)-ATP; KN-62, 1-[N,O-bis(5-isoquinolinesulphonyl)-N-methyl-L-tyrosyl]-4-phenylpiperazine; MRS 2159, 4-[(4-formyl-5-hydroxy-6-methyl-3-[(phosphonooxy)methyl}-2-pyridinyl)azo]-benzoic acid; PPADS, pyridoxal phosphate-6-azophenyl-2-4-disulphonic acid; PPNDS, pyridoxal-5′-phosphate-6-(2′-naphthylazo-6′-nitro-4′,8′-disulphonate).

Table 3 Activities of P2 receptor antagonists to block BzATP-stimulated changes in intracellular calcium concentrations

Antagonist	*Mouse P2X7, BALB/c (pIC$_{50}$)*	*Mouse P2X7, C57BL/6 (pIC$_{50}$)*	*Rat P2X7 (pIC$_{50}$)*	*Human P2X7 (pIC$_{50}$)*
PPADS	4.39 ± 0.07	4.31 ± 0.06	5.08 ± 0.02	5.49 ± 0.03
KN-62	<4	<4	<4	4.97 ± 0.12
BBG	<4	<4	5.09 ± 0.06	<4
PPNDS	5.10 ± 0.09	4.96 ± 0.03	6.03 ± 0.01	6.39 ± 0.02
MRS 2159	4.80 ± 0.05	4.73 ± 0.04	5.33 ± 0.04	5.76 ± 0.03
NF279	4.80 ± 0.30*	<4	<4	4.70 ± 0.05
A-740003	6.57 ± 0.04	6.17 ± 0.05	7.74 ± 0.02	7.36 ± 0.01
A-438079	6.01 ± 0.12	6.26 ± 0.07	6.51 ± 0.03	6.91 ± 0.01

Data represent pIC_{50} ± SEM, n = 4–6 individual experiments. The concentration of BzATP used for each species was equivalent to the EC_{70} agonist concentration (μmol·L^{-1}) and was 150 (BALB/c), 150 (C57BL/6), 10 (rat) and 5 (human). The following antagonists did not significantly inhibit BzATP-mediated changes in intracellular calcium concentrations at concentrations up to 100 μmol·L^{-1}: suramin, Cibacron Blue, NF023, NF449, MRS 2179, A-317491, TNP-ATP, Reactive Blue, phenol red, caffeine, theophylline, mecamylamine and oATP (tested at 1 mmol·L^{-1}). Data for A-740003 and A-438079 at human P2X7 receptors are from Honore *et al.* (2006) and Nelson *et al.* (2006) respectively.
BBG, Brilliant Blue G; BzATP, 2,3-O-(4-benzoylbenzoyl)-ATP; KN-62, 1-[N,O-bis(5-isoquinolinesulphonyl)-N-methyl-L-tyrosyl]-4-phenylpiperazine; MRS 2159, 4-[(4-formyl-5-hydroxy-6-methyl-3-[(phosphonooxy)methyl}-2-pyridinyl)azo]-benzoic acid; MRS 2179, 2′deoxy-N^6-methyl adenosine 3′,5′-diphosphate; oATP, periodate oxidized ATP; PPADS, pyridoxal phosphate-6-azophenyl-2-4-disulphonic acid; PPNDS, pyridoxal-5′-phosphate-6-(2′-naphthylazo-6′-nitro-4′,8′-disulphonate); TNP-ATP, 2′,3′-O-(2,4,6-trinitrophenyl) adenosine 5′-triphosphate.
*Maximal antagonist activity for NF279 at BALB/c P2X7 receptors was 59%.

A-438079 maintained high potency to block rat and human P2X7 receptors at both preincubation times (Table 5).

Selectivity of P2 receptor antagonists

Because several reported P2X1 receptor antagonists were found to be potent blockers of mammalian P2X7 receptor-mediated calcium influx and Yo-Pro uptake (Tables 3 and 4), the activity of these antagonists was assessed at other human P2 receptors including P2X1, P2X2, P2X2/3, P2X4, P2Y1 and P2Y2 (Table 6). PPNDS, MRS 2159, NF279 and PPADS showed similar potency to block several P2 receptor subtypes including P2X1, P2X2, P2X2/3 and P2X7. In contrast, A-740003 and A-438079 selectively blocked only P2X7 receptors (Honore *et al.*, 2006; McGaraughty *et al.*, 2007). NF449 selectively blocked P2X1 receptor-mediated changes in intracellular calcium concentrations. None of these compounds significantly inhibited P2X4-mediated calcium influx (Table 6).

As extending the calcium influx assay incubation time increased the potency of these antagonists to block P2X7 receptors, PPNDS, MRS 2159, NF279, NF449 and PPADS were

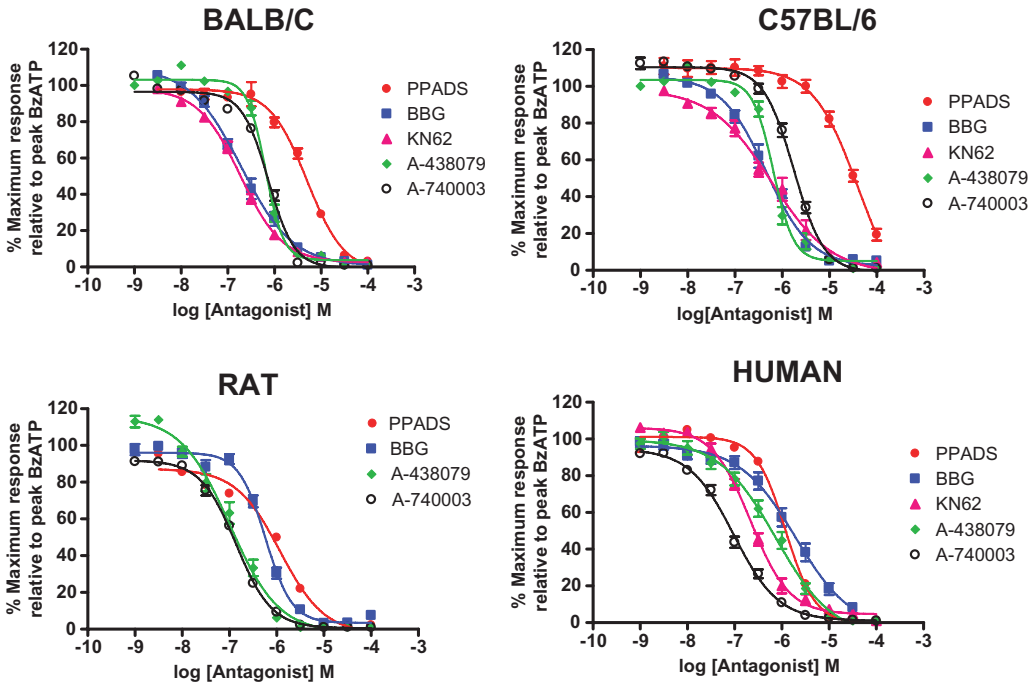

Figure 5 Concentration–effect curves for P2 receptor antagonists to block BzATP-stimulated Yo-Pro uptake. Data were normalized to the peak BzATP response (%Maximum response). Data represent mean ± SEM of 4–6 experiments. BBG, Brilliant Blue G; BzATP, 2,3-O-(4-benzoylbenzoyl)-ATP; KN-62, 1-[N,O-bis(5-isoquinolinesulphonyl)-N-methyl-L-tyrosyl]-4-phenylpiperazine; PPADS, pyridoxal phosphate-6-azophenyl-2-4-disulphonic acid.

Table 4 Activities of P2 receptor antagonists to block P2X7 receptor-mediated Yo-Pro uptake

Antagonist	*Mouse P2X7, BALB/c* (pIC_{50})	*Mouse P2X7, C57BL/6* (pIC_{50})	*Rat P2X7* (pIC_{50})	*Human P2X7* (pIC_{50})
PPADS	5.31 ± 0.08	4.40 ± 0.02	5.93 ± 0.07	5.92 ± 0.03
KN-62	6.73 ± 0.07	6.23 ± 0.09	<4	6.67 ± 0.07
BBG	6.71 ± 0.05	6.34 ± 0.08	6.24 ± 0.06	5.71 ± 0.13
Cibracon Blue	5.57 ± 0.06	5.41 ± 0.21	5.18 ± 0.06	5.14 ± 0.29
PPNDS	6.05 ± 0.03	6.02 ± 0.06	6.26 ± 0.07	6.70 ± 0.04
MRS 2159	5.49 ± 0.10	5.36 ± 0.12	6.04 ± 0.07	6.54 ± 0.05
NF023	5.79 ± 0.16	5.49 ± 0.21	5.66 ± 0.07	4.92 ± 0.07
NF279	6.11 ± 0.07	6.14 ± 0.05	5.98 ± 0.15	6.05 ± 0.08
NF449	6.25 ± 0.03	6.07 ± 0.04	5.96 ± 0.09	5.83 ± 0.06
Reactive Blue	4.67 ± 0.07	4.75 ± 0.26	5.55 ± 0.04	5.27 ± 0.04
A-740003	6.14 ± 0.04	5.76 ± 0.03	7.00 ± 0.02	7.03 ± 0.04
A-438079	6.19 ± 0.03	6.19 ± 0.04	6.99 ± 0.06	6.03 ± 0.30

Data represent pIC_{50} ± SEM, n = 4–6 individual experiments. The concentration of BzATP used for each species was equivalent to the EC_{70} agonist concentration (in $\mu mol \cdot L^{-1}$) and was 90 (BALB/c), 90 (C57BL/6), 15 (rat) and 2.5 (human). The following antagonists did not significantly inhibit BzATP-mediated Yo-Pro uptake at concentrations up to 100 $\mu mol \cdot L^{-1}$: suramin, MRS 2179, A-317491, TNP-ATP, caffeine, theophylline, mecamylamine and oATP (tested at 1 $mmol \cdot L^{-1}$). Data for A-740003 and A-438079 at human P2X7 receptors are from Honore *et al.* (2006) and Nelson *et al.* (2006) respectively.
BBG, Brilliant Blue G; BzATP, 2,3-O-(4-benzoylbenzoyl)-ATP; KN-62, 1-[N,O-bis(5-isoquinolinesulphonyl)-N-methyl-L-tyrosyl]-4-phenylpiperazine; MRS 2159, 4-[(4-formyl-5-hydroxy-6-methyl-3-[(phosphonooxy)methyl}-2-pyridinyl)azo]-benzoic acid; MRS 2179, 2′deoxy-N^6-methyl adenosine 3′,5′-diphosphate; oATP, periodate oxidized ATP; PPADS, pyridoxal phosphate-6-azophenyl-2-4-disulphonic acid; PPNDS, pyridoxal-5′-phosphate-6-(2′-naphthylazo-6′-nitro-4′,8′-disulphonate); TNP-ATP, 2′,3′-O-(2,4,6-trinitrophenyl) adenosine 5′-triphosphate.

evaluated for pharmacological selectivity at P2X1, P2X2, P2X2/3 and P2X7 under both the short (3 min) and long (60 min) assay incubation times (Table 7). Similar to that for P2X7 receptors, increasing assay incubation times enhanced the potency of these antagonists to block P2X receptors. However, extension of the assay incubation time did not significantly alter the relative pharmacological selectivity of these compounds (Table 7). With the exception of NF449, which blocked only P2X1 receptors, all other compounds non-selectively blocked the other P2X receptors (Table 7).

Discussion

High concentrations of ATP are required to activate P2X7 receptors (North, 2002). Channel activation results in

Table 5 Activities of P2 receptor antagonists to block P2X7 receptor-mediated changes in intracellular calcium concentrations

Antagonist	*Mouse P2X7, BALB/c*	*Mouse P2X7, C57BL/6*	*Rat P2X7*	*Human P2X7*
PPADS, 3 min	4.39 ± 0.07	4.31 ± 0.06	5.08 ± 0.02	5.49 ± 0.03
PPADS, 60 min	4.83 ± 0.05	4.69 ± 0.02	5.71 ± 0.04	6.33 ± 0.02
KN-62, 3 min	<4	<4	<4	4.97 ± 0.12
KN-62, 60 min	6.41 ± 0.02	6.44 ± 0.05	<4	6.42 ± 0.02
BBG, 3 min	<4	<4	5.09 ± 0.06	<4
BBG, 60 min	5.73 ± 0.03	5.76 ± 0.01	6.16 ± 0.03	<4
PPNDS, 3 min	5.10 ± 0.09	4.96 ± 0.03	6.03 ± 0.01	6.39 ± 0.02
PPNDS, 60 min	5.66 ± 0.02	5.40 ± 0.03	6.45 ± 0.02	6.63 ± 0.02
MRS 2159, 3 min	4.80 ± 0.05	4.73 ± 0.04	5.33 ± 0.04	5.76 ± 0.03
MRS 2159, 60 min	5.40 ± 0.02	5.37 ± 0.03	6.00 ± 0.02	6.53 ± 0.02
NF279, 3 min	4.80 ± 0.05*	<4	<4	4.70 ± 0.05
NF279, 60 min	5.84 ± 0.08*	<4	4.65 ± 0.05	5.22 ± 0.04
Reactive Blue, 3 min	<4	<4	<4	<4
Reactive Blue, 60 min	4.21 ± 0.09	4.48 ± 0.13	<4	4.49 ± 0.33
A-740003, 3 min	6.57 ± 0.04	6.17 ± 0.05	7.74 ± 0.02	7.36 ± 0.01
A-740003, 60 min	6.26 ± 0.04	6.48 ± 0.03	7.92 ± 0.04	7.28 ± 0.03
A-438079, 3 min	6.01 ± 0.12	6.26 ± 0.07	6.51 ± 0.03	6.91 ± 0.01
A-438079, 60 min	5.61 ± 0.03	5.86 ± 0.05	6.32 ± 0.05	7.50 ± 0.08

Data represent pIC_{50} ± SEM, n = 4–6 individual experiments. Agonist concentrations for each species are indicated in Table 3. The following agonists did not produce a significant change in intracellular calcium concentrations at concentrations up to 1 mmol·L^{-1}: Cibacron Blue, NF023, NF449, oATP and phenol red when preincubated for either 3 or 60 min. Data (3 min) for A-740003 and A-438079 at human and rat P2X7 receptors are from Honore *et al.* (2006) and Nelson *et al.* (2006) respectively.

BBG, Brilliant Blue G; KN-62, 1-[N,O-bis(5-isoquinolinesulphonyl)-N-methyl-L-tyrosyl]-4-phenylpiperazine; MRS 2159, 4-[(4-formyl-5-hydroxy-6-methyl-3-[(phosphonooxy)methyl}-2-pyridinyl)azo]-benzoic acid; oATP, periodate oxidized ATP; PPADS, pyridoxal phosphate-6-azophenyl-2-4-disulphonic acid; PPNDS, pyridoxal-5′-phosphate-6-(2′-naphthylazo-6′-nitro-4′,8′-disulphonate).

*Maximal antagonist activity for NF279 at BALB/c P2X7 receptors was 59% at 3 min and 64% at 60 min.

Table 6 Activity of selected P2 receptor antagonists in blocking human P2 receptor-mediated changes in intracellular calcium concentrations

Antagonist	*Human P2X1* (pIC_{50})	*Human P2X2* (pIC_{50})	*Human P2X2/3* (pIC_{50})	*Human P2X4* (pIC_{50})	*Human P2X7* (pIC_{50})	*Human $P2Y_1$* (pIC_{50})	*Human $P2Y_2$* (pIC_{50})
PPNDS	5.66 ± 0.10	5.77 ± 0.04	5.59 ± 0.04	<4	6.39 ± 0.02	5.44 ± 0.25	4.84 ± 0.11
MRS 2159	5.26 ± 0.08	5.20 ± 0.04	5.02 ± 0.04	<4	5.76 ± 0.03	4.69 ± 0.10	<4
BBG	<4	<4	<4	<4	<4	<4	<4
NF279	5.06 ± 0.08	4.59 ± 0.06	<4	<4	4.70 ± 0.05	4.68 ± 0.09	<4
NF449	6.21 ± 0.05	<4	<4	<4	<4	<4	<4
PPADS	5.89 ± 0.36	4.69 ± 0.08	4.78 ± 0.15	<4	5.49 ± 0.03	5.70 ± 0.11	<4
A-740003	<4	<4	<4	<4	7.36 ± 0.01	<4	<4
A-438079	<4	<4	<4	<4	6.91 ± 0.01	<4	<4

Data represent pIC_{50} ± SEM, n = 4–6 individual experiments. Assay parameters were identical to those described by Bianchi *et al.* (1999). None of the antagonists tested showed any significant inhibitory activity at human P2X4 receptors at concentrations up to 100 μmol·L^{-1}. Data for A-740003 and A-438079 at human P2X7 receptors are from Honore *et al.* (2006) and Nelson *et al.* (2006) respectively.

BBG, Brilliant Blue G; MRS 2159, 4-[(4-formyl-5-hydroxy-6-methyl-3-[(phosphonooxy)methyl}-2-pyridinyl)azo]-benzoic acid; PPADS, pyridoxal phosphate-6-azophenyl-2-4-disulphonic acid; PPNDS, pyridoxal-5′-phosphate-6-(2′-naphthylazo-6′-nitro-4′,8′-disulphonate).

Table 7 Effect of extended pretreatment time on the relative selectivity of several P2X1 receptor antagonists to block receptor-mediated calcium influx

Antagonist	*P2X1* (pIC_{50})	*P2X2* (pIC_{50})	*P2X2/3* (pIC_{50})	*P2X7* (pIC_{50})
PPNDS, 3 min	5.66 ± 0.10	5.77 ± 0.04	5.59 ± 0.04	6.39 ± 0.03
PPNDS, 60 min	6.80 ± 0.04	5.69 ± 0.04	6.07 ± 0.05	6.63 ± 0.02
MRS 2159, 3 min	5.26 ± 0.09	5.20 ± 0.04	5.02 ± 0.04	5.76 ± 0.03
MRS 2159, 60 min	6.69 ± 0.04	5.63 ± 0.03	5.73 ± 0.06	6.53 ± 0.02
NF279, 3 min	5.06 ± 0.08	4.59 ± 0.06	<4	4.70 ± 0.05
NF279, 60 min	5.43 ± 0.55	4.55 ± 0.34	<4	5.22 ± 0.04
NF449, 3 min	6.21 ± 0.05	<4	<4	<4
NF449, 60 min	6.50 ± 0.23	<4	<4	<4
PPADS, 3 min	5.89 ± 0.35	4.69 ± 0.08	4.78 ± 0.15	5.49 ± 0.03
PPADS, 60 min	5.88 ± 0.05	5.70 ± 0.08	5.25 ± 0.09	6.33 ± 0.02

Data represents pIC_{50} ± SEM, n = 4–6 individual experiments. Data represents pIC_{50} ± SEM, n = 4–6 individual experiments. Assay parameters were identical to those described by Bianchi *et al.* (1999).

MRS 2159, 4-[(4-formyl-5-hydroxy-6-methyl-3-[(phosphonooxy)methyl}-2-pyridinyl)azo]-benzoic acid; PPADS, pyridoxal phosphate-6-azophenyl-2-4-disulphonic acid; PPNDS, pyridoxal-5′-phosphate-6-(2′-naphthylazo-6′-nitro-4′,8′-disulphonate).

immediate cationic permeability and, following more prolonged activation, permeability of large (~900 Da) molecules (North, 2002). Activation of P2X7 receptors also leads to cytoskeletal and mitochondrial alterations including actin/α-tublin rearrangement, phosphatidylserine translocation, mitochrondrial swelling, maturation and release of IL-1β and membrane blebbing (Liu *et al.*, 2008; Roger *et al.*, 2008). Further, P2X7-mediated pore formation involves multiple signalling pathways that include a rapid recruitment of Panx-1 hemichannels and a slower maitotoxin-like mechanism (Pelegrin and Surprenant, 2006; 2007). Thus, P2X7 receptors represent a multifunctional pro-inflammatory purinoceptor that may serve as a danger signal during tissue trauma (Ferrari *et al.*, 2006).

The present data provide a systematic analysis of mammalian P2X7 receptor pharmacology by using two well-characterized P2X7 receptor-mediated effects, changes in intracellular calcium concentrations and Yo-Pro uptake (North, 2002; Burnstock, 2007; Donnelly-Roberts and Jarvis, 2007). These data clearly demonstrate that a reported loss of function P451L mutation found in C57BL/6 mice (Adriouch *et al.*, 2002) is fully functional when expressed in 1321N1 cells. Furthermore, C57BL/6 mouse P2X7 receptors show a nearly identical *in vitro* pharmacological profile to the BALB/c mouse P2X7 receptor when expressed in 1321N1 cells.

This study confirms and extends the differential agonist activity of BzATP and ATP at human and rat P2X7 receptors (Surprenant and North, 2009). While several previous studies have examined the molecular basis for species differences in P2X7 receptor agonist pharmacology using stably transfected HEK-293 cells (Hibell *et al.*, 2001a,b; Michel *et al.*, 2008), an advantage of the present data is the use of 1321N1 cells that do not natively express functional P2X receptors (Bianchi *et al.*, 1999). HEK-293 cells natively express P2Y1 and P2Y2 receptors (Schachter *et al.*, 1997). Furthermore, transient expression systems using both mammalian and non-mammalian host cells have produced variable results in investigations of P2X7-mediated pore formation (North, 2002; Liu *et al.*, 2008). Consequently, the use of P2X7 expressing 1321N1 cells allows for simultaneous investigation of agonist evoked channel opening (e.g. calcium influx) and pore formation (Yo-Pro uptake) (Bianchi *et al.*, 1999; Donnelly-Roberts *et al.*, 2004). Both the apparent potency and relative efficacy of agonists can be clearly attributed to activation of P2X7 receptors using this null background cell line (Bianchi *et al.*, 1999).

Overall, BzATP was the most potent agonist in evoking calcium influx at human, rat and mouse P2X7 receptors. ATP, in contrast, was a significantly weaker agonist compared with BzATP and showed partial agonist activity at the rat P2X7 receptor. 2MeSATP and ATPγS showed weak or no agonist activity at rat and mouse P2X7 receptors. The relative differences in agonist potency for BzATP and ATP on calcium influx were also seen for P2X7 receptor-mediated Yo-Pro uptake and are consistent with previous studies using both recombinant and native receptor systems (Chen *et al.*, 2005; Anderson and Nedergaard, 2006). While 2MeSATP was a weakly potent full agonist in stimulating human P2X7 receptor-mediated calcium flux, it was completely ineffective in stimulating Yo-Pro uptake. Thus, the differential activity of agonists for mammalian P2X7 receptors may be mediated by a recently reported difference in amino acid homology in the ectodomain between species (Young *et al.*, 2007). In addition, differences in agonist potencies across species could be the result of differences in the rates by which agonists are able to modulate channel kinetics (Hibell *et al.*, 2001a,b).

The present data also provide several new insights regarding the antagonist pharmacology of mammalian P2X7 receptors. A common feature of previously identified P2X7 receptor antagonists including KN-62, BBG, PPADS and oATP is their differential affinity for human versus rat P2X7 receptors (Anderson and Nedergaard, 2006; Donnelly-Roberts and Jarvis, 2007; Michel *et al.*, 2007). For example, KN-62 (Humphreys *et al.*, 1998) potently blocks human P2X7 receptors, but lacks activity at the rat receptor. While the present data confirm this species difference between human and rat P2X7 receptors, KN-62 effectively blocked mouse P2X7 receptor pore formation. Interestingly, the reported P2X1 receptor-selective antagonist, NF279 (Klappertstuck *et al.*, 2000; Rettinger *et al.*, 2000; 2005), was more effective in blocking human than rat or mouse P2X7 receptor-mediated calcium influx.

Other recently reported adamantine-based antagonists including AZ116453743 (Stokes *et al.*, 2006) compound 17 (Michel *et al.*, 2007) show a significant reduction in potency at the rat receptor relative to human P2X7 receptors. These antagonists, as well as others (e.g. NF279, NF449, PPADS, BBG and oATP) have slow association rates and do not competitively block agonist activation of P2X receptors (Burnstock, 2007; Michel *et al.*, 2007). In contrast, two recently described P2X7 receptor antagonists from different chemical classes, A-740003 and A-438079 (Honore *et al.*, 2006; Nelson *et al.*, 2006), show a high degree of selectivity for blocking P2X7 receptors and competitively block P2X7 receptors with pA_2 values of 7.0 and 6.9 respectively (Honore *et al.*, 2006; Nelson *et al.*, 2006). By virtue of their increase affinity for blocking P2X7 receptors, these newer antagonists tend to show less species differences compared with the other compounds evaluated (e.g. KN-62, BBG and NF279) in this study. Another distinguishing feature of these selective P2X7 receptor antagonists is their similar affinity for blocking P2X7 receptor-mediated calcium influx, pore formation and IL-1β release (Honore *et al.*, 2006; Donnelly-Roberts and Jarvis, 2007).

As the two functional consequences of P2X7 receptor activation, calcium influx and pore formation differ in their temporal patterns (North, 2002; Surprenant and North, 2009), additional experiments were conducted to assess calcium influx antagonist pharmacology following a 60 min incubation as was done in the pore formation assay. Consistent with their slow kinetics, many antagonists showed enhanced potency with extended incubation times. However, increasing antagonist incubation times did not significantly alter the relative P2X receptor selectivity for non-selective antagonists. A-740003 and A-438079 showed less time-dependent changes in potency compared with the other antagonists studied and showed equivalent affinities for blocking P2X7 receptor-mediated calcium influx and pore formation. Thus, A-740003 and A-438079 appear to function as high-affinity and selective P2X7 receptor antagonists, regardless of the P2X7

receptor-mediated physiological end point. The mechanism(s) for the differential ability of other, less selective antagonists to block P2X7 receptor-mediated calcium influx and pore formation remains unknown. The present data do not rule out the possibility that some of these antagonists may interfere with downstream signalling mechanisms associated with P2X7 receptor-stimulated recruitment of hemichannels to the cell surface (Pelegrin and Surprenant, 2006; 2007).

It is interesting that many of the reported loss of function mutations for the P2X7 receptor are localized on the intracellular C-terminus (North, 2002). This region of the P2X7 receptor is essential for receptor-mediated pore formation (Surprenant *et al.*, 1996; North, 2002; Surprenant and North, 2009) and serves as a common end point measured in P2X7 receptor single-nucleotide polymorphism studies (Donnelly-Roberts and Jarvis, 2007). However, as it has recently been shown that the formation of large pores in the cell membrane following P2X7 receptor activation is dependent on multiple signalling mechanisms including recruitment of hemichannels to the cell surface (Pelegrin and Surprenant, 2006; 2007), it is likely that not all cells possess the necessary intracellular components to generate large pores (North, 2002; Pelegrin and Surprenant, 2006; Donnelly-Roberts and Jarvis 2007). While the exact reasons for differences in the functionality of C57BL/6 and BALB/c mouse P2X7 receptors that were reported by Adriouch *et al*. (2002) compared with the present results are unknown, BzATP-evoked calcium responses in mouse splenic T cells were detected in both C57BL/6 and BALB/c mice in the Adriouch *et al*. (2002) study. Variations in the level of T cell P2X7 receptor expression and other methodological disparities may account for a differential magnitude of P2X7 receptor-mediated responses in these mouse strains. This apparent difference in P2X7 receptor functionality may also be modulated by differential intracellular signalling mechanisms involved in the recruitment of hemichannels to the cell surface (Iglesias *et al.*, 2008). Nevertheless, the present data show that when both mouse P2X7 receptors are expressed at comparable levels in 1321N1 cells, similar agonist-evoked calcium influx and Yo-Pro uptake responses and agonist and antagonist pharmacological profiles were found.

In summary, the present data provide the first direct comparison of the pharmacological profiles of P2 antagonists across mouse, rat and human P2X7 receptors expressed in the same host cell line. These data should serve as a useful guide for the study of P2X7 receptors in *in vivo* studies.

Note added in proof

For a comprehensive review of the current structure activity relationships for P2X7 receptor antagonists, see Guile SD *et al*. (2009) J Med Chem DOI: 1021/jm801528x.

Conflicts of interest

All authors are employees of Abbott Laboratories and have no conflicts of interest.

References

Adriouch S, Dox C, Welge V, Seman M, Koch-Nolte F, Haag F (2002). Cutting Edge: a natural P451L mutation in the cytoplasmic domain impairs the function of the mouse P2X7 receptor. *J Immunol* **169**: 4108–4112.

Alexander SPH, Mathie A, Peters JA (2008). Guide to receptors and channels (GRAC), 3rd edn. *Br J Pharmacol* **153** (Suppl. 2): S1–S209.

Anderson CM, Nedergaard M (2006). Emerging challenges of assigning P2X(7) receptor function and immunoreactivity in neurons. *Trends Neurosci* **29**: 257–262.

Bianchi BR, Lynch KJ, Touma E, Niforatos W, Burgard EC, Alexander KM *et al*. (1999). Pharmacological characterization of recombinant human and rat P2X receptor subtypes. *Eur J Pharmacol* **376**: 127–138.

Burnstock G (2007). Physiology and pathophysiology of purinergic neurotransmission. *Physiol Rev* **87**: 659–797.

Chen Y-W, Donnelly-Roberts D, Gintant G, Cox B, Jarvis MF, Harris R (2005). Pharmacological characterization of P2X7 receptors in rat peritoneal cells. *Inflamm Res* **54**: 119–126.

Chessell IP, Hatcher J, Bountra C, Michel AD, Hughes JP, Green P *et al*. (2005). Disruption of the P2X7 purinoceptor gene abolishes chronic inflammatory and neuropathic pain. *Pain* **114**: 386–396.

Denlinger LC, Fisette PL, Sommer JA, Watters JJ, Prabhu U, Dubyak GR *et al*. (2001). The nucleotide receptor P2X7 contains multiple protein- and lipid- interaction motifs including a potential binding site for bacterial lipopolysaccharide. *J Immunol* **167**: 1871–1876.

Donnelly-Roberts DL, Jarvis MF (2007). Discovery of P2X7 receptor-selective antagonists offers new insights into P2X7 receptor function and indicates a role in chronic pain states. *Br J Pharmacol* **151**: 571–579.

Donnelly-Roberts DL, Namovic M, Faltynek CR, Jarvis MF (2004). Mitogen-activated protein kinase and caspase signaling pathways are required for P2X7 receptor (P2X7R)-induced pore formation in Human THP-1 cells. *J Pharmacol Exp Ther* **308**: 1053–1061.

Dubyak GR (2007). Go it alone no more-P2X7 joins the society of heteromeric ATP-gated receptor channels. *Mol Pharmacol* **72**: 1402–1405.

Ferrari D, Pizzirani C, Adinolfi E, Lemoli RM, Curti A, Idzko M *et al*. (2006). The P2X7 receptor: a key player in IL-1 processing and release. *J Immunol* **176**: 3877–3883.

Gargett CE, Wiley JS (1997). The isoquinoline derivative KN-62 is a potent antagonist of the $P2X_Z$-receptor of human lymphocytes. *Br J Pharmacol* **120**: 1483–1490.

Hibell AD, Tompson KM, Simon M, Xing M, Humphrey PPA, Michel AD (2001a). Species and agonist-dependent differences in the deactivation-kinetics of $P2X_7$ receptors. *Naunyn Schmiedebergs Arch Pharmacol* **363**: 639–648.

Hibell AD, Thompson KM, Xing M, Humphrey PPA, Michel AD (2001b). Complexities of measuring antagonist potency at P2X7 receptor orthologs. *J Pharmacol Exp Ther* **296**: 947–957.

Honore PM, Donnelly-Roberts D, Namovic M, Hsieh G, Zhu C, Mikusa J *et al*. (2006). A-740003 (N-(1-{[(cyanoimino)(5-quinolinylamino) methyl]amino}-2,2-dimethylpropyl)-2-(3,4-dimethoxyphenyl) acetamide, a novel and selective P2X7 receptor antagonist dose-dependently reduces neuropathic pain in the rat. *J Pharmacol Exp Ther* **319**: 1376–1385.

Humphreys BD, Virginio C, Surprenant A, Rice J, Dubyak GR (1998). Isoquinolines as antagonists of the P2X7 nucelotide receptor: high selectivity for the human versus rat receptor. *Mol Pharmacol* **54**: 22–32.

Iglesias R, Locovei S, Roque A, Alberto AP, Dahl G, Spray DC *et al*. (2008). P2X7 receptor-pannexin1 complex: Pharmacology and signaling. *Am J Physiol Cell Physiol* **295**: C752–C760.

Jacobson KA, Jarvis MF, Williams M (2002). Perspective: purine and pyrimidine. (P2) receptors as drug targets. *J Med Chem* **45**: 4057–4093.

Jarvis MF, Khakh BS (2009). ATP-gated cation channels. *Neuropharmacology* **56**: 208–215.

Jiang LH, MacKenzie AB, North RA, Surprenant A (2000). BBG selectively blocks ATP-gated rat P2X7 receptors. *Mol Pharmacol* **58**: 82–88.

Kassack MU, Braun K, Ganso M, Ullmann H, Nickel P, Boing B *et al*. (2004). Structure-activity relationships of analogues of NF449 confirm NF449 as the most potent and selective known P2X1 receptor antagonist. *Eur J Med Chem* **39**: 345–357.

Kim M, Jiang LH, Wilson HL, North RA, Suprenant A (2001). Proteomic and functional evidence for a P2X7 receptor signaling complex. *EMBO J* **20**: 6347–6358.

Klappertstuck M, Buttner C, Nickel P, Schmalzing G, Lambrecht G, Markwardt F (2000). Antagonism by the suramin analogue NF279 on human P2X1 and P2X7 receptors. *Eur J Pharmacol* **387**: 245–252.

Labasi JM, Petrushova N, Donovan C, McCurdy S, Lira P, Payette MM *et al*. (2002). Absence of the P2X7 receptor alters leukocyte function and attenuates an inflammatory response. *J Immunol* **168**: 6436–6445.

Lambrecht G (2000). Agonists and antagonists acting at P2X receptors: selectivity profiles and functional implications. *Naunyn Schmiedebergs Arch Pharmacol* **362**: 340–350.

Le Stunff H, Auger L, Kanellopoulous J, Raymond M-N (2004). The Pro-451 to Leu polymorphism within the C-terminal tail of P2X7 receptor impairs cell death but not phospholipase D activation in murine thymocytes. *J Biol Chem* **279**: 16918–16926.

Liu X, Surprenant A, Mao H-J, Roger S, Xia R, Bradley H *et al*. (2008). Identification of key residues coordinating functional inhibition of P2X7 recpetors by zinc and copper. *Mol Pharmacol* **73**: 252–259.

Lynch KJ, Touma E, Niforatos W, Kage KL, Burgard EC, van Biessen T *et al*. (1999). Molecular and functional characterization of human P2X(2) receptors. *Mol Pharmacol* **56**: 1171–1181.

McGaraughty S, Chu KL, Namovic MT, Donnelly-Roberts DL, Harris RR, Zhang X-F, Shieh C-C *et al*. (2007). P2X7-related modulation of pathological nociception in rats. *Neuroscience* **146**: 1817–1828.

Michel AD, Chambers IP, Humphrey PPA (2007). Direct labeling of the human P2X7 receptor and identification of positive and negative cooperativity of binding. *Br J Pharmacol* **151**: 103–114.

Michel AS, Clay WC, Ng SW, Roman S, Thompson K, Condreay JP *et al*. (2008). Identification of regions of the p2X7 receptor that contribute to human and rat species differences in antagonist effects. *Br J Pharmacol* **155**: 738–751.

Nelson DW, Gregg RJ, Kort ME, Perez-Medrano A, Voight EA, Wang Y *et al*. (2006). Structure-activity relationship studies on a series of novel, substituted 1-Benzyl-5-phenyltetrazole P2X7 antagonists. *J Med Chem* **49**: 3659–3666.

North AR (2002). Molecular physiology of P2X receptors. *Physiol Rev* **82**: 1013–1067.

Pelegrin P, Surprenant A (2006). Pannexin-1 mediates large pore formation and interleukin-1b release by the ATP-gated P2X7 receptor. *EMBO J* **25**: 5071–5082.

Pelegrin P, Surprenant A (2007). Pannexin-1 couples to maitotoxin- and nigericing-induced interleukin-1β release through a dye uptake-independent pathway. *J Biol Chem* **282**: 2386–2394.

Rassendren F, Buell GN, Newbolt A, North RA, Surprenant A (1997). Identification of amino acid residues contributing to the pore of a P2X receptor. *EMBO J* **16**: 3446–3454.

Rettinger J, Schmalzing G, Damer S, Muller G, Nickel P, Lambrecht G (2000). The surmanin analogue NF279 is a novel and potent antagonist selective for the P2X(1) receptor. *Neuropharmacology* **39**: 2044–2053.

Rettinger J, Braun K, Hochmann H, Kassack MU, Ullmann H, Nickel P *et al*. (2005). Profiling at recombinant homomeric and heteromeric rat P2X receptors identifies the suramin analogue NF449 as a highly potent P2X1 receptor antagonist. *Neuropharmacology* **48**: 461–468.

Roger S, Pelegrin P, Surprenant A (2008). Facilitation of P2X7 receptor currents and membrane blebbing via constitutive and dynamic calmodulin binding. *J Neurosci* **28**: 6393–6401.

Sanz JM, DiVirgilio F (2000). Kinetics and mechanism of ATP-dependent IL-1β release from microglia cells. *J Immunol* **164**: 4893–4898.

Schachter JB, Sromek AM, Nicholas RA, Harden TK (1997). HEK293 human embryonic kidney cells endogenously express the P2Y1 and P2Y2 receptors. *Neuropharmacology* **36**: 1181–1187.

Solle M, Labasi J, Perregaux DG, Stam E, Petrushova N, Koller BH *et al*. (2001). altered cytokine production in mice lacking P2X7 receptors. *J Biol Chem* **276**: 125–132.

Stokes L, Jiang L-H, Alcaraz L, Bent J, Bowers K, Fagura M *et al*. (2006). Characterization of a selective and potent antagonist of human P2X7 receptors, AZ11645373. *Br J Pharmacol* **149**: 880–887.

Surprenant A, North RA (2009). Signaling at purinergic P2X receptors. *Annu Rev Physiol* **71**: 333–359.

Surprenant A, Rassendren F, Kawashima E, North RA, Buell G (1996). The cytolytic P2z receptor for extracellular ATP identified as a P2X receptor (P2X7). *Science* **272**: 735–738.

Young M, Pelegrin P, Surprenant A (2007). Amino acid residues in the P2X7 receptor that mediate differential sensitivity to ATP and BzATP. *Mol Pharmacol* **71**: 92–100.